FULL RESEARCH PAPER

Temporal dynamics of pathogenesis-related metabolites and their plausible pathways of induction in potato leaves following inoculation with *Phytophthora infestans*

**Y. Abu-Nada · A. C. Kushalappa ·
W. D. Marshall · K. Al-Mughrabi · A. Murphy**

Abstract Metabolite profiles based on GC/MS were used to study the temporal dynamics of metabolites in potato leaves following pathogen inoculation. In the polar and non-polar plant extracts a total of 106 consistent peaks were detected, of which 95 metabolites were tentatively identified. Following pathogen inoculation, the abundances of 42 metabolites were significantly increased or decreased, and these metabolites were designated as Pathogenesis-Related (PR) Metabolites. Factor analysis of the abundance of 106 metabolites identified four plant–pathogen interaction functions: (i) homeostasis; (ii) primary defence; (iii) secondary defence; (iv) collapse of primary and secondary defence responses. During the primary and secondary defence phases, dramatic changes in the amino acids, known precursors of several plant defence-related metabolites, were observed. Plausible satellite-networks of metabolic pathways leading to the up-regulation of these families of amino acids and other secondary metabolites, and their potential application for the evaluation of horizontal resistance in potato against the late blight pathogen is discussed.

Abbreviations

GC/MS	gas chromatography/mass spectrometry
P R - metabolites	pathogenesis-related metabolites, up (PRU) or down (PRD) regulated.

Y. Abu-Nada · A. C. Kushalappa (✉)
Department of Plant Science, McGill University, Ste. Anne de Bellevue, Montreal, QC, Canada, H9X 3V9
e-mail: ajjamada.kushalappa@mcgill.ca

W. D. Marshall
Department of Food Science and Agriculture Chemistry, McGill University, Ste. Anne de Bellevue, Montreal, QC, Canada, H9X 3V9

K. Al-Mughrabi
New Brunswick Department of Agriculture, Wicklow, NB, Canada, E7L 3S4

A. Murphy
Agriculture and Agri-Food Canada, Fredericton, NB, Canada, E3B 4Z7

Introduction

Late blight, caused by *Phytophthora infestans*, is one of the most destructive diseases of potato (Flier et al. 2003). *Phytophthora infestans* is a heterothallic pathogen that requires both A1 and the A2 mating types for sexual reproduction (Daayf and Platt 1999; Peters et al. 1999; Stromberg et al. 2001). In Canada, the clonal lineage US-8 (A2 mating type) is the most

aggressive and dominant on cultivated potato culti-vars (Daayf and Platt 2003; Medina et al. 1999; Peters et al. 2001). Systemic fungicides are used extensively to manage this disease and have led to the development of resistant populations. Accordingly, the use of resistant cultivars is considered the best option to manage this disease.

Breeding for vertical resistance is easier than horizontal resistance. At least 11 vertical resistance R genes against *P. infestans* have been introduced into cultivated potato from the wild potato *Solanum demissum* (Gebhardt and Valkonen 2001; Wastie 1991). Unfortunately, vertical resistance is not as durable as the horizontal resistance, thus is the current focus of many breeding programmes (Peters et al. 1999; Simmonds and Wastie 1987). However, breeding for horizontal resistance in potato is difficult because it is controlled by several genes (Evers et al. 2003). The quantitative resistance in potato against the late blight is generally measured based on multiple epidemiological disease parameters such as latent period, lesion size, and amount of sporulation (Carlisle et al. 2002). However, these techniques are not only time-consuming but also cannot explain the mechanism of resistance. Metabolic profiling is an alternative tool for breeders for high throughput phenotyping of resistance.

Plants defend abiotic and biotic stresses through development of structural barriers and production of chemical compounds such as signal molecules and phytoalexins (Kombrink and Schmelzer 2001; Montesano et al. 2003; Osbourn 1996). Following pathogen invasion plants produce pathogenesis-related proteins (PR-proteins) (Palva et al. 1993) and pathogenesis-related metabolites (PR-metabo-lites) (Hamzehzarghani, et al. 2005). Even though the plant genes, transcripts and proteins, are ex-pressed following pathogen attack, the metabolomics approach will enhance our knowledge concerning the functions of genes. Therefore, metabolomics should be included as an integral part of functional genom-ics, for a comprehensive understanding of the plant–pathogen interaction (Bino et al. 2004; Fiehn 2001; Sumner et al. 2003). Accordingly, metabolite profil-ing has been used to discriminate genetically mod-ified traits (Munger et al. 2005; Roessner et al. 2001), growth of potato microtubers in vitro and in soil (Roessner et al. 2000), homozygous ecotypes from single gene mutants in *Arabidopsis thaliana* (Fiehn

et al. 2000b), wheat cultivars varying in resistance against fusarium head blight disease (Hamzehzar-ghani et al. 2005), *Medicago truncatula* exposed to biotic and abiotic stress factors (Broeckling et al. 2005), and salt-stressed from non-stressed tomatoes (Johnson et al. 2003).

Phytophthora infestans is a hemibiotroph, where in a compatible plant–pathogen interactions, the pathogen begins its invasion as a biotroph by penetrating the host epidermal cells in about 16 h and producing haustoria in about 22 h. Around 46 h, the pathogen is well established in the host, becomes a necrotroph and starts producing sporangia (Vlees-houwers et al. 2000). Therefore, it would be very interesting to see if the temporal dynamics of metabolites following pathogen invasion, can lead to a better understanding of pathogenicity. The objective of this study was to use a metabolomics approach to study the temporal dynamics of metab-olites and their plausible pathways of production with the advance in pathogenesis following inoculation with *P. infestans*.

Materials and methods

Potato plant production

Elite seed tubers of the potato cv. AC Novachip were obtained from the Potato Research Centre, Agricul-ture and Agri-Food Canada, New Brunswick. Tubers were planted in 16 cm diam pots (one tuber per pot) containing mixture of 1:1 ratio of soil and PRO-Mix BX$^{®}$ (Premier Horticulture Ltd, Riviere-du-Loup, QC) and maintained at 20°C, 16 h photoperiod and around 70% RH on a growth bench. Plants were fertilized weekly with 200 ml pot^{-1} of a solution (1.5 g l^{-1}) of Plant-Prod$^{®}$ 20:20:20 containing trace elements (Plant Products Co. Ltd., Ontario, Canada); 1–3 stems per plant/pot were maintained.

Pathogen

Phytophthora infestans (clonal lineage US-8, A2 mating type, isolate (1661) was obtained from AAFC, Charlottetown, PEI. The pathogen was sub-cultured on Rye-Agar media at 15°C. After 2–3 weeks a sporangial suspension was made with sterilized water

containing 0.02% Tween 80. The concentration of sporangia in the suspension was adjusted to 1.0×10^5 sporangia ml^{-1}.

Inoculation and incubation

Three days before inoculation, 5–6 week old plants grown on growth benches were transferred to a growth chamber maintained at 20°C, 16 h photoperiod and 90% RH. Six completely developed leaflets, from 1–3 stems of a single-tuber plant, were inoculated at two sites, once on each side of the midrib, with 5 μl of the sporangial suspension. The plants were misted with sterile water, covered with plastic bags to maintain high RH, and transferred back to the growth chamber. The bags were removed 24 h after inoculation.

Disease severity and sporulation assessment

The diameter of lesions was measured at 2, 4, 6, and 8 days after inoculation, from which the lesion area was calculated; 24 h after inoculation leaf discs containing inoculation sites were cut using an 18 mm diam cork borer. Ten discs were transferred to a Petri dish lined with moist sterile filter paper and incubated at 20°C and 16 h photoperiod. After 6 days, they were transferred to a test tube containing 4 ml aqueous solution of 0.02% Tween 80 and vortexed. The number of sporangia was determined using a hemacytometer and represented as number of sporangia per leaf disc/inoculation site.

Metabolite extraction and GC/MS analysis

Leaf discs containing the inoculation sites were cut using a 15 mm cork borer, treated with liquid nitrogen and stored at −80°C for a few days, lyophilized for 48 h and returned to storage at −80°C until extraction. The polar and non-polar metabolites were extracted following methods developed by Fiehn et al. (2000 a,b) with minor modifications. The lyophilized tissue was first crushed in liquid nitrogen and the polar metabolites were extracted from a 30 mg sample using 1.4 ml methanol and 50 μl water. To the same sample, 50 μl ribitol (0.2 mg ml^{-1} water) and 50 μl nonadecanoic acid methyl ester (2 mg ml^{-1} chloroform) were added as internal standards. The samples were heated at 70°C for 15 min and centrifuged at 13,500 rpm for 3 min. The supernatant was transferred to a glass tube with a screw cap with teflonized inlays; 1.4 ml pure water was added. For the non-polar pellets, 0.75 ml chloroform was added, vortex and heated at 37°C with continuous shaking for 5 min. Samples were centrifuged at 13,500 rpm for 3 min. The non-polar supernatant and the previously obtained water/methanol extract were mixed together, vortexed and centrifuged at 3,800 rpm for 15 min. The upper polar phase was decanted into another tube and filtered through 15 ml Millipore tubes. One ml of this extract was dried using a Speed Vac., and 50 μl of methoxyamine hydrochloride (20 mg ml^{-1} pyridine) was added to the dried sample. The samples were heated with continuous shaking at 30°C for 90 min and derivatized by adding 80 μl of MSTFA and heating for 30 min at 37°C. Samples were kept at 25°C for 2 h before injection into the GC/MS; 1 μl of the sample was injected into GC/MS with a split ratio of 1:25. The lower portion, the non-polar chloroform-phase, was transferred to a new vial and 0.90 ml of chloroform and 1 ml of methanol containing 3% v/v H_2SO_4 were added. Lipids and free fatty acids found in samples were transmethylated for 4 h at 100°C. Each sample was cleaned twice by adding 4 ml pure water, vortexed and centrifuged at 3800 rpm for 15 min. The water phase was discarded and anhydrous sodium sulphate was added to the remaining non-polar extract to remove excess water. The supernatant was transferred to a new glass tube and dried by using Speed Vac; 80 μl of chloroform was added to dissolve the dried metabolites. The samples were derivatized and silylated by adding 10 μl MSTFA and 10 μl pyridine at 37°C for 30 min; 1 μl of the sample was injected into the GC/MS with a split ratio of 1:5. Before injection in to the GC/MS, the Lee's retention time index standards (chrysene, naphthalene, and phenanthrene) were added to both polar and non-polar samples (Eckel 2000).

GC/MS analysis

Samples were transferred to an auto sampler that injected 1 μl into the GC injection port (model 2100 T, Varian®, Canada) connected to a GC/MS (GC 3400XC with Voyager® ion trap mass analyzer; Varian ®, QC, Canada). The GC was equipped with a

capillary column (30 m DB-5MS column with 0.25 mm diam, 0.25 μm film thick, Supelco, Canada). The injection port was heated to 230°C. Helium was used as a carrier gas with a flow rate of 1 ml s^{-1}. The oven was programmed at 70°C for 5 min and then increased at a rate of 5°C min^{-1} until 290°C, where it was held for 6 min. The mass spectra from 45 to 600 m/z were recorded using an ion trap analyzer. Data were analyzed using Saturn Lab Software. The GC/MS data consisted of scans and abundances (the ion trap detector output that measures the signal intensity, ion current, for each of the ion fragments detected during the scan and is proportional to the concentration of metabolites) of mass ions.

Data processing

The GC/MS outputs on abundances of mass ions at different scans were imported into spreadsheet and organized using the Pivot Table Procedures of the EXCEL$^{®}$ programme. The consistency of mass ion spectra of peaks, with about the same retention time, in five replicates of each treatment was inspected using SATURN Lab software (SATURN $^{®}$ GC/MS workstation version 5.52), and the most probable choice of a name was selected for the compound using NIST (National Institute of Standards and Technology, MD, USA) and/or SATURN libraries. Some peaks, even though consistent, had low probability matches. These were designated as unidentified and their spectra (m/z) in decreasing order of relative abundance were given instead of names. Metabolites that were not consistent among replicates were excluded from further analysis.

The Lee Retention Index (RI) (Lee et al. 1979) was calculated for all the metabolites (Eckel 2000) using the formula: RI = { 100 × (RT$_{unknown}$ − RT$_n$)/(RT$_{n+1}$ − RT$_n$)} + 100(n), where RT$_{unknown}$ is the Retention Time of the unknown metabolite; the RT$_n$ and RT$_{n+1}$ are the retention time of the standards that eluted before and after the unknown, respectively; (n) represents the number of rings of the aromatic hydrocarbon standards, that is 2 for naphthalene, 3 for phenanthrene and 4 for chrysene. The Lee RI was also used to confirm or to refuse the compound names, proposed by automated mass spectral search libraries, based on the boiling point in degrees Celsius of a metabolite, which is always greater than its RI for metabolites smaller than

Hexacosane (Eckel 2000). Metabolites with boiling points (obtained from SciFinder$^{®}$ Scholar Version 2002, American Chemical Society) less than their RI were considered unknown. The tentatively identified metabolites were grouped according to their biological functions. The metabolite spectra were further compared with Golm Metabolome Database (http://csbdb.mpimp-golm.mpg.de/csbdb/gmd/gmd.html) (Kopka et al. 2005).

Experimental design and data analysis

Three experiments were conducted simultaneously: (1) metabolite profiling: the experiment was designed as a randomized complete block with four treatments: water inoculated and incubated for 24 h (W1 = Control), and pathogen inoculated and incubated for 24 h (P1), 48 h (P2) and 96 h (P4). The entire block was repeated 5 times, over time, thus 5 replicates. Each experimental unit consisted of 12-leaflet discs cut from six inoculated leaflets of a single-tuber plant. Each experimental unit consisted of a pool of metabolites from polar (methanol-water) and non-polar (chloroform) extracts analyzed separately using GC/MS. (2) Disease severity assessment: the experiment was designed as a randomized complete block design with one treatment of pathogen inoculation and conducted 5 times, thus 5 blocks. Each experimental unit consisted of measurements (over time) of 12 inoculated sites in six leaflets from a single-tuber-plant. (3) sporulation assessment: the experiment was a completely randomized design with one treatment and 5 replicates. Each experimental unit consisted of 10 inoculation sites in five leaflets from a single-tuber plant.

The data on abundances of metabolites were subjected to analysis of variance using ANOVA procedure of SAS to identify the compounds significantly different among treatments and Duncan's multiple range tests at ($p = 0.05$) was used to compare the different treatments (Khattree and Naik 2000). The metabolites that were significantly up or down-regulated following pathogen inoculation, relative to water inoculation, were identified. The abundances of 106 metabolites were further subjected to FACTOR procedure of SAS, using principle component and the orthogonal (VARIMAX) rotational methods, to identify the contribution (factor-loading) of each metabolite to a treatment and the relationships among

treatments based on a spatial location of treatments in scatter plot of factor-scores for significant factors (Johnson and Wichern 2002; Hamzehzarghani et al. 2005). The factor-scores classified the treatments (scatter plot) and the classes separated by factor-vectors were related to disease progress to identify plant–pathogen interaction functions, which in turn were explained using sets of metabolites with high factor loadings to the respective factors. A positive factor-score was associated with positive factor-loadings of a set of metabolites. The factor-loading of a compound increased with an increase in its abundance in a treatment relative to other treatments.

The data on disease severity (average lesion area in mm^2) and sporulation (number of spores lesion^{-1}) were subjected to ANOVA using SAS programme.

Results

Disease severity and amount of sporulation

The average lesion areas 2, 4, and 6 days after inoculation (DAI) were 77.8, 114.3, and 124.5 mm^2, respectively. The average number of sporangia at 6 DAI was 5.33×10^3 disc^{-1}.

Temporal dynamics of metabolites

Homeostasis and PR-metabolites

Metabolite profiling detected more than 300 peaks; however, only a total of 106 peaks were consistent in all the 5 replicates and had abundances $>2 \times 10^3$, including 36 from the chloroform phase and 70 from the methanol–water phase. Among the consistent metabolites, 95 were tentatively identified including 14 amino acids (AAs), 21 fatty acids (FAs), 24 organic acids (OAs), 19 sugars (SRs) and 17 belonging to other groups (O). The remaining 11 metabolites were unidentified (Table 1). According to ANOVA tests of 106 metabolites, the abundances of 42 metabolites were significantly different ($P < 0.05$) among treatments (W1, P1, P2 and P4). The abundances of most of these metabolites increased following pathogen inoculation, meaning the ratios of abundances of compounds between Pathogen/Water (P/W-ratio) inoculated were >1.0.

The metabolites significantly increased or decreased after the pathogen inoculation were designated as PR metabolites, either up (PRU) or down (PRD)-regulated, respectively (Table 1).

The temporal dynamics of PR-metabolites within functional groups

The PR-metabolites consisted of 9 AAs, 10 OAs, 9 FAs, 4 SRs, 3 belonging to other groups (O) and 7 were unidentified.

Several AAs and OAs were up-regulated in the first two days after pathogen infection (P1 and P2). In P1, 8 PRU-metabolites were found including L-aspartic acid (1 = serial numbers of compounds in Table 1), L-threonine (2), L-alanine (3), L-proline (4), L-valine (5), L-isoleucine (6), L-tyrosine (7), and Glutamine (8) (Table 1). In P2, 6 PRU-metabolites including L-threonine (2), L-valine (5), L-isoleucine (6), L-tyrosine (7) Glutamine (8) and L-phenylalanine (9) were detected. In P4, all the AAs were not significantly different from the WI except for the PRU-metabolite Glutamine (8). Generally, in P1 members of 4 of the AAs families were activated. In P2, L-tyrosine and L-phenylalanine, aromatic AAs, and L-threonine (2), L-isoleucine (6), members of aspartic acid family, were noticeably up-regulated compared to W treatment. In P4, the abundances of all the 9 AAs belonging to the 4 families except glutamine (8) were not significantly different from W treatment.

Ten organic acids were found to be PR-metabolites. In P1, 4 PRU-metabolites including Butanoic acid (15), propanetricarboxylic acid (16 = Isocitric acid), trihydroxypentanoic acid (17), and galactonic acid (19) were detected. In P2, 6 PRU-metabolites were detected including trihydroxypentanoic acid (17), trihydroxybutyric acid (18), galactonic acid (19), 2-Keto-l-gluconic acid (20), tetronic acid (21), and D-Gluconic acid (22). In P4, 5 OAs were PRU-metabolites including galactonic acid (19), 2-Keto-l-gluconic acid (20), tetronic acid (21), D-Gluconic acid (22), L-Gluconic acid (24) and 1 PRD-metabolite, dihydroxybutanoic acid (23), were found.

Three fatty acids were up-regulated in P1, namely Hexadecanoic acid (39 = Palmitic acid), 9,12-Octadecadienoic acid (40 = Linoleic acid), and 9-Octadecanoic acid (41 = Oleic acid). In P2, 3

Table 1 Metabolites and their abundances ($\times 10^6$) (W) or ratio (P/W) detected in leaves of potato cultivar AC Novachip at different incubation times after inoculation with the pathogen *P. infestans* (P) or water (W)

No.[1]	RI[1]	Metabolite Name[2]	CAS[3]	Group[4]	W[5]	P1/W[6]	P2/W	P4/W	F1[7]	F2	F3
1	258.1	L-Aspartic acid, N-(trimethylsilyl)-, (GN)	55268-53-6	AA	1.24^B	2.50^A	1.67^B	1.03^B	0.12	0.88	0.46
2	234.7	N,O,O-Tris(trimethylsilyl)-L-threonine (GN)	7537-02-2	AA	0.36^C	3.04^A	2.09^B	1.27^{BC}	0.04	0.88	0.48
3	229.6	EIQTMS_N12C......L-Alanine (3TMS) (G)	N/A	AA	0.71^B	1.77^A	0.81^B	0.38^B	0.61	0.78	0.15
4	257.6	L-Proline, 5-oxo-1-(trimethylsilyl)-, tri (NG)	30274-77-2	AA	1.77^{BC}	1.60^A	1.22^{AB}	0.71^C	0.48	0.76	0.45
5	203.9	L-Valine, N-(trimethylsilyl)-, trimeth (NG)	7364-44-5	AA	0.54^B	2.68^A	2.21^A	1.19^B	0.01	0.73	0.68
6	219.4	L-Isoleucine, N-(trimethylsilyl), tri (NG)	7483-92-3	AA	0.24^B	3.43^A	3.29^A	2.60^B	−0.52	0.63	0.57
7	324.5	L-Tyrosine, N,O-bis(trimethylsilyl)-, tri (NG)	51220-73-6	AA	0.24^B	2.36^A	2.62^A	1.31^B	−0.12	0.49	0.86
8	274.6	Glutamine, tris(trimethylsilyl)-(GN)	15985-07-6	AA	0.32^B	2.47^A	2.96^A	2.33^A	−0.63	0.38	0.68
9	274.8	N,O-Bis(trimethylsilyl)-L-phenylalanine (GN)	7364-51-4	AA	0.42^B	1.51^{AB}	1.82^A	1.43^{AB}	−0.56	0.26	0.79
10	230.3	L-Serine, N,O-bis(trimethylsilyl)-, tr (GN)	7364-48-9	AA	0.73	2.88	2.22	2.04	−0.40	0.84	0.36
11	184.0	L-Alanine, N-(trimethylsilyl (NG)	27844-07-1	AA	1.28	1.98	1.66	1.45	−0.35	0.83	0.43
12	220.1	L-Proline, 1-(trimethylsilyl)-, trimeth (NG)	7364-47-8	AA	0.11	1.89	1.99	1.74	−0.59	0.52	0.62
13	221.0	Glycine, N,N-bis(trimethylsilyl)-, tri (GN)	5630-82-0	AA	0.58	1.12	1.01	1.37	−0.79	0.20	−0.58
14	282.3	TMS 1-TMS-5-TMSoxy-3-(2-TMSamino (N)	69937-47-9	AA	1.09	0.61	0.63	0.71	0.58	−0.60	−0.55
15	259.1	Butanoic acid, 4-[bis(trimethylsilyl) (NG)	39508-23-1	OA	4.49^B	1.53^A	1.23^B	1.12^B	−0.01	0.94	0.33
16	293.3	1,2,3-Propanetricarboxylic acid, 2-(N)	14330-97-3	OA	0.77^B	1.50^A	1.31^{AB}	1.01^B	0.13	0.84	0.52
17	278.9	EIQTMS_N12 trihydroxypentanoic acid (G)	N/A	OA	0.44^B	1.37^A	1.26^A	1.18^{AB}	−0.35	0.82	0.45
18	264.8	2,3,4-Trihydroxybutyric acid tetraTMS(N)	38191-88-7	OA	0.88^B	1.34^{AB}	1.52^A	1.14^B	−0.25	0.43	0.87
19	333.5	Galactonic acid, 2,3,4,5,6-pentaki (GN)	55400-16-3	OA	0.10^C	1.64^B	1.96^A	1.60^B	−0.68	0.32	0.66
20	296.2	2-Keto-1-gluconic acid, penta(trim (GN)	N/A	OA	0.21^B	1.28^B	1.60^A	1.69^A	−0.95	0.05	0.29
21	261.8	EIQTMS_N12C_LJARL_1574 tetronic acid (G)	N/A	OA	0.13^C	1.17^C	1.72^B	2.11^A	−0.98	−0.17	0.08
22	330.3	D-Gluconic acid, 2,3,4,5,6-pentakis (N)	34290-52-3	OA	0.08^B	1.12^B	1.48^A	1.69^A	−0.98	−0.20	0.08
23	243.3	(R*,S*)-3,4-Dihydroxybutanoic acid (N)	55191-53-2	OA	0.08^A	0.76^{AB}	0.74^{AB}	0.59^B	0.95	−0.30	−0.06
24	299.1	L-Gluconic acid, 2,3,5,6-tetrakis-O (N)	56298-43-2	OA	0.23^{BC}	0.85^C	1.07^B	1.32^A	−0.81	−0.54	−0.24
25	228.9	2-Butenedioic acid (E)-, bis(trime (GN)	17962-03-7	OA	0.35	1.12	0.87	0.99	0.24	0.74	−0.63
26	222.4	Butanedioic acid, bis(trimethylsilyl) (GN)	40309-57-7	OA	1.39	1.11	0.91	0.95	0.64	0.74	−0.20
27	168.9	Butanedioic acid, 2,3-bis[(trimethyls (N)	57456-93-6	OA	2.74	1.32	1.32	1.01	−0.02	0.59	0.81
28	291.9	Arabinoic acid, 2,3,5-tris-O-(trimeth (N)	10589-37-4	OA	0.20	1.17	1.14	0.90	0.45	0.58	0.68
29	179.6	Acetic acid, [(trimethylsilyl)oxy]-, (N)	33581-77-0	OA	1.33	1.31	1.31	1.32	−0.87	0.44	0.23
30	304.5	1-Cyclohexene-1-carboxylic a (N)	55520-78-0	OA	0.36	1.29	1.57	0.99	−0.01	0.18	0.98
31	263.6	á-Amino isobutyric acid tri-TMS II (N)	N/A	OA	0.07	0.97	0.92	0.81	0.97	0.04	0.22
32	305.7	1-Propene-1,2,3-tricarboxylic acid, (N)	55530-71-7	OA	5.28	0.83	0.74	0.55	1.00	−0.05	0.00

Table 1 continued

No.	RI[1]	Metabolite Name[2]	CAS[3]	Group[4]	W[5]	P1/W[6]	P2/W	P4/W	F1[7]	F2	F3
33	176.7	Propanoic acid, 2-[(trimethylsilyl) (NG)	17596-96-2	OA	5.08	0.89	0.89	0.72	0.97	−0.15	0.21
34	224.6	Propanoic acid, 2,3-bis[(trimethylsi (NG)	38191-87-6	OA	4.23	0.92	1.45	1.96	−0.93	−0.36	−0.12
35	249.4	3-Hydroxy glutaric acid tri-TMS (N)	N/A	OA	0.34	0.81	0.79	0.71	0.91	−0.38	−0.13
36	231.9	Erythro-Pentonic acid, 2-deoxy-3,4, (N)	74742-30-6	OA	0.17	0.67	0.75	0.54	0.91	−0.41	0.05
37	267.6	Pentanedioic acid, 2-(methoxyimi (N)	60022-87-9	OA	0.26	0.74	0.67	0.75	0.62	−0.41	−0.67
38	294.5	Ribonic acid, 2,3,4,5-tetrakis-O-(tr (NG)	57197-35-0	OA	0.13	0.93	1.19	1.16	−0.74	−0.62	0.25
39	323.3	Hexadecanoic acid, methyl ester (N)	112-39-0	FA	7.12^B	1.19^A	1.08^AB	1.03^B	0.05	0.93	0.37
40	349.0	9,12-Octadecadienoic acid (Z,Z) (NG)	112-63-0	FA	8.33^BC	1.23^A	1.06^B	0.92^C	0.41	0.81	0.42
41	350.8	9-Octadecenoic acid (Z)-, methyl (N)	112-62-9	FA	0.11^C	1.50^A	1.45^AB	1.19^BC	−0.26	0.75	0.61
42	322.3	9-Hexadecenoic acid, methyl ester, (N)	1120-25-8	FA	0.60^A	1.07^A	0.96^B	0.80^B	0.80	0.50	0.33
43	350.0	9,12,15-Octadecatrienoic acid, (GN)	301-00-8	FA	16.96^AB	1.06^A	0.87^B	0.66^C	0.89	0.39	0.23
44	318.3	7,10,13-Hexadecatrienoic acid, me (N)	56554-30-4	FA	2.04^A	1.02^A	0.76^B	0.47^C	0.92	0.38	0.10
45	317.5	7,10-Hexadecadienoic acid, meth (N)	16106-03-9	FA	0.25^A	1.04^A	0.71^B	0.45^C	0.93	0.36	0.08
46	328.7	Hexadecanoic acid (N)	57-10-3	FA	0.23^B	1.50^B	2.46^A	1.06^B	−0.15	0.02	0.99
47	382.1	Eicosanoic acid, methyl ester (NG)	1120-28-1	FA	0.90^B	1.10^AB	1.23^A	1.24^A	−0.92	−0.01	0.40
48	338.8	Heptadecanoic acid, methyl ester (NG)	1731-92-6	FA	0.26	1.11	0.98	0.98	0.23	0.97	0.01
49*	291.0	Tridecanoic acid, 12-methyl-, meth (N)	5129-58-8	FA	0.18	1.30	1.12	1.14	−0.20	0.96	0.20
50	370.4	Octadecanoic acid, trimethylsilyl (NG)	18748-91-9	FA	1.27	1.17	1.20	0.99	0.06	0.57	0.82
51	415.0	Hexadecanoic acid, 2,3-bis[(trime (N)	1188-74-5	FA	0.27	4.76	5.27	5.64	−0.84	0.42	0.34
52	437.7	Octadecanoic acid, 2,3-bis[(trime (N)	1188-75-6	FA	1.42	3.13	3.48	4.03	−0.91	0.33	0.25
53	341.7	Hexadecanoic acid, trimethylsilyl (NG)	55520-89-3	FA	0.88	1.22	1.45	0.94	0.05	0.21	0.98
54	354.0	Octadecanoic acid, methyl ester (GN)	112-61-8	FA	7.73	1.01	1.05	0.98	0.09	−0.03	1.00
55*	334.4	Hexadecanoic acid, 14-methyl-, m (N)	2490-49-5	FA	0.25	1.02	1.12	1.09	−0.74	−0.09	0.66
56*	432.3	Tetracosanoic acid, methyl ester (N)	2442-49-1	FA	0.52	0.98	0.99	1.10	−0.73	−0.24	−0.64
57*	510.2	Triacontanoic acid, methyl ester (N)	629-83-4	FA	0.63	0.98	1.30	0.88	0.14	−0.25	0.96
58*	408.0	Docosanoic acid, methyl ester (N)	929-77-1	FA	0.62	0.98	1.14	1.21	−0.89	−0.46	0.09
59*	420.4	Tricosanoic acid, methyl ester (N)	2433-97-8	FA	0.13	0.89	0.99	1.21	−0.71	−0.57	−0.40
60	322.9	D-Mannitol, 1,2,3,4,5,6-hexakis-O-(N)	14317-07-8	SR	0.14^AB	1.12^A	0.96^B	0.70^C	0.86	0.40	0.32
61	347.6	Myo-Inositol, 1,2,3,4,5,6-hexakis-O (GN)	2582-79-8	SR	0.81^A	0.95^AB	0.77^BC	0.66^C	0.97	0.23	−0.09
62	268.0	Xylulose tetra-TMS (GN)	N/A	SR	0.36^C	1.29^BC	1.70^AB	2.14^A	−0.99	−0.10	0.04
63	362.7	D-Glucose, 4-O-[2,3,4,6-tetrakis-O (N)	55669-93-7	SR	0.20^A	0.69^B	0.67^B	0.54^B	0.93	−0.31	−0.21
64	281.1	D-Ribofuranose, 1,2,3,5-tetrakis-O-(tr (N)	56271-69-3	SR	0.14	1.38	1.17	1.04	0.00	0.95	0.32
65	283.4	á-D-Galactofuranoside, ethyl 2,3,5, (N)	55493-81-7	SR	0.71	1.28	1.22	1.02	0.02	0.71	0.70

Table 1 continued

No.	RI[1]	Metabolite Name[2]	CAS[3]	Group[4]	W[5]	P1/W[6]	P2/W	P4/W	F1[7]	F2	F3
66	315.5	D-Fructose, 1,3,4,5,6-pentakis-O-(tri (N)	56196-14-6	SR	11.44	1.03	0.87	0.66	0.85	0.46	0.26
67	317.9	Glucose oxime hexaTMS (N)	120850-89-7	SR	12.87	0.98	0.81	0.72	0.91	0.37	−0.18
68	280.0	Arabinofuranose, 1,2,3,5-tetrakis-O (N)	55399-49-0	SR	0.29	1.30	1.42	0.97	0.06	0.33	0.94
69	320.8	Galactose oxime hexaTMS (NG)	120850-88-6	SR	2.29	0.97	0.83	0.69	0.98	0.20	0.02
70	285.3	à-L-Mannopyranose, 6-deoxy-1,2,3, (N)	55057-21-1	SR	0.09	1.23	1.48	1.11	−0.29	0.18	0.94
71	297.3	.beta.-DL-Arabinopyranose, 2 (N)	56271-64-8	SR	0.50	1.03	1.09	0.86	0.57	0.07	0.82
72	339.1	D-Altrose, 2,3,4,5,6-pentakis-O-(trim (N)	56114-56-8	SR	0.10	1.07	1.03	1.14	−0.90	−0.03	−0.43
73	420.9	à-D-Glucopyranoside, 1,3,4,6-tetra (N)	19159-25-2	SR	0.52	1.24	1.55	1.66	−0.96	−0.07	0.27
74	260.8	Mannofuranoside, methyl 2,3,5,6-(N)	6737-01-5	SR	0.40	0.85	0.83	0.76	0.95	−0.27	−0.13
75	289.2	EIQTMS_N12C_SD1_1727.8_1215BK1 (G)	N/A	SR	0.13	0.81	0.81	0.74	0.94	−0.33	−0.05
76	235.4	á-D-Galactopyranoside, methyl 2,3-(N)	56211-10-0	SR	0.11	0.66	0.73	0.71	0.69	−0.66	−0.30
77	255.0	à-D-Galactopyranoside, methyl 2 (N)	56196-94-2	SR	0.56	0.62	0.77	0.62	0.73	−0.68	−0.04
78	292.7	D-Xylofuranose, 1,2,3,5-tetrakis-O-(tr (N)	56271-68-2	SR	0.59	0.84	0.98	0.98	−0.13	−0.98	−0.15
79	473.1	Solanid-5-en-3-ol, (3à)-(N)	80-78-4	O(G)	0.42^B	2.17^A	2.13^A	1.70^A	−0.45	0.63	0.64
80	310.0	3,7,11,15-Tetramethyl-2-hexadecen (N)	102608-53-7	O(AA)	0.17^{AB}	1.13^A	0.73^B	0.67^B	0.83	0.55	−0.06
81	337.9	Silanamine, 1,1,1-trimethyl-N-(trim (GN)	55556-99-5	O(P)	0.09^C	1.44^B	1.97^A	1.08^C	−0.15	0.07	0.99
82*	311.5	3,5-Cyclohexadiene-1,2-dione, 3,5 (N)	3383-21-9	O(DQ)	0.44	1.38	1.11	1.33	−0.57	0.80	−0.21
83	319.5	Propionic aldehyde, 2',3,3,4',5' (N)	N/A	O(Q)	0.62	1.44	1.15	1.40	−0.61	0.77	−0.20
84	260.9	2,4,6-Tri-t-butylbenzenethiol (GN)	961-39-7	O(SC)	0.33	1.05	0.95	0.94	0.74	0.62	−0.25
85	271.2	Trimethylsilyl ether of glycerol (NG)	6787-10-6	O(AA)	0.15	1.51	1.52	0.96	0.15	0.55	0.82
86	471.1	Stigmastan-3,5-dien (N)	N/A	O(S)	0.42	1.48	1.47	1.81	−0.95	0.30	0.01
87	210.8	Benzene, 1,3-bis(1,1-dimethylethyl (NG)	1014-60-4	O(AH)	0.21	1.16	1.20	1.22	−0.86	0.29	0.41
88	493.1	á-Sitosterol acetate (N)	915-05-9	O(S)	2.93	1.18	1.24	1.38	−0.97	0.23	0.06
89	496.1	Stigmasterol trimethylsilyl ether (NG)	14030-29-6	O(S)	1.09	1.11	1.11	1.19	−0.97	0.23	−0.09
90	247.1	Putrescine tetraTMS (GN)	39772-63-9	O(NC)	1.18	0.99	0.99	0.88	0.82	0.14	0.55
91	248.8	2,5-Cyclohexadiene-1,4-dione, 2,6 (N)	719-22-2	O(DQ)	0.18	1.12	1.17	1.23	−1.00	0.08	0.02
92	190.6	Cystathionine-diTMS (N)	73090-79-6	O(AAD)	1.00	0.94	0.75	0.98	0.22	0.06	−0.97
93	287.1	Nonadecane (N)	629-92-5	O(AK)	0.15	1.08	1.20	0.98	−0.09	0.01	1.00
94	506.3	á-Sitosterol trimethylsilyl ether (NG)	2625-46-9	O(S)	1.34	1.00	1.18	1.24	−0.92	−0.36	0.15
95	467.4	Cholest-5-ene, 3-methoxy-, (3à)-(N)	1174-92-1	O(S)	0.34	0.67	1.23	1.10	−0.39	−0.87	0.29
96	299.6	Unidentified (73,288,147,74,361)	N/A	N/A	3.63^B	1.48^A	1.16^B	0.95^B	0.27	0.88	0.38
97	242.0	Unidentified (174,73,175,155,86)	N/A	N/A	0.56^B	1.38^A	1.32^A	0.90^B	0.26	0.59	0.77
98	313.6	Unidentified (123,81,95,278,96)	N/A	N/A	0.38^A	1.06^A	0.72^B	0.65^B	0.84	0.51	−0.20

Table 1 continued

No.	RI[1]	Metabolite Name[2]	CAS[3]	Group[4]	W[5]	P1/W[6]	P2/W	P4/W	F1[7]	F2	F3
99	167.9	Unidentified (73,89,147,59,161)	N/A	N/A	5.62^{BC}	1.15^{AB}	1.19^A	0.94^C	0.20	0.42	0.88
100	458.7	Unidentified (193,73,119,105,147)	N/A	N/A	1.30^B	1.39^{AB}	1.99^A	1.83^A	−0.85	−0.06	0.52
101	240.5	Unidentified (189,73,221,147,174)	N/A	N/A	0.21^A	0.80^B	0.75^{BC}	0.64^C	0.96	−0.23	−0.15
102	253.0	Unidentified (73,333,147,265,407)	N/A	N/A	42.96^A	0.64^B	0.66^B	0.65^B	0.72	−0.57	−0.39
103	262.6	Unidentified (247,249,173,175,145)	N/A	N/A	0.20	1.25	1.30	1.09	−0.15	0.46	0.87
104	311.6	Unidentified (346,347,73,74,345)	N/A	N/A	2.80	1.12	1.14	0.85	0.46	0.31	0.83
105	313.9	Unidentified (218,73,217,74,147)	N/A	N/A	15.71	1.05	0.89	0.67	0.93	0.26	0.25
106	284.2	Unidentified (290,73,217,234,304)	N/A	N/A	0.25	0.80	0.86	0.85	0.63	−0.69	−0.36

* Metabolites having Boiling Points < Lee Retention Index but had high match probabilities in the libraries

1 Retention Index (RI), calculated based on Eckel (2000)

2 Shortened names according to NIST (N = a letter in parenthesis at the end of the name) or Golm Metabolome Database (G) or both (NG); libraries with higher probability for the same metabolite are listed first

3 CAS Registry Number = Chemical Abstract Service Registry Number

4 Chemical groups of compounds: AA = Amino Acid; FA = Fatty Acid; OA = Organic Acid; O(AA) = Other Aliphatic Alcohol; O(AAD) = Other amino acid derivatives; O(AH) = Other Aromatic Hydrocarbon; O(D) = Other Diene; O(P) = Other Phenolic; O(DQ) = Other Diene Quinone; O(G) = Other Glykoalkaloids; O(Q) = Other Quinone; O(S) = Other Steroid; O(SC) = Other Sulphur containing; Sugar = SR

5 Total abundance (×10^6) of Water-inoculated plants (control)

6 The metabolite regulation ratio = pathogen inoculated over water inoculated (P/W > 1.0 is up-regulated; P/W < 1.0 is down-regulated) at 1, 2 and 4 DAI; different letters indicate significance at $p = 0.05$ by comparing the means of the total abundance of the four treatments using Duncan's multiple range test

7 Factor-loadings of metabolites to F1, F2 and F3-scores, based on factor analysis of abundances of 106 metabolites; the loadings can be positive or negative.

PRU-metabolites and 3 PRD-metabolites were detected, namely 9-Octadecanoic acid (41), Hexadecanoic acid (46), Eicosanoic acid (47), 9-Hexadecenoic acid (42), 7,10,13-Hexadecatrienoic acid (44), 7,10-Hexadecadienoic acid (45), respectively. In P4, 1 PRU-metabolite Eicosanoic acid (47) and 4 PRD-metabolites namely, 9-Hexadecenoic acid (42), 9,12,15-Octadecatrienoic acid (43), 7,10,13-Hexadecatrienoic acid (44), and 7,10-Hexadecadienoic acid (45) were found. Generally, the total abundances of the unsaturated FAs were reduced with the progress of the disease P4 < P2 < P1.

Among sugars and in P1, only D-Glucose (63) was a PRD-metabolite. In P2, one PRU-metabolite, Xylulose (62) and two PRD-metabolites, Myo-Inositol (61) and D-Glucose (63) were detected. In P4, 1 PRU-metabolite, Xylulose (62) and 3 PRD-metabolites, D-Mannitol (60), Myo-Inositol (61) and D-Glucose (63) were found.

Among other groups, Solanidine (79) was found to be a PRU-metabolite in P1, P2 and P4.

Two unidentified metabolites PRU-metabolites (96 and 97) and 2 PDR-metabolites (101, 102) were found in P1. In P2, 3 PRU-metabolites 97, 99, 100 and 3 PRD-metabolite 98, 101 and 102 were detected. In general, two PRD-metabolites 101 and 102 were found in P1, P2 and P4 treatments.

Factor-loadings of metabolites to factor vectors and their plausible plant defence phases

The FACTOR analysis of abundances of 106 metabolites was used to classify the treatments and to identify the biological functions underneath the separation of classes. The first three factors explained 100% of the total variance (F1 = 45.56%, F2 = 27.47% and F3 = 26.97%). The scatter plot, using factor-scores for the first three factors, discriminating four treatments (W1, P1, P2 and P4) is shown in Fig. 1. Factor-loadings of different metabolites to each of the three factors are shown as a list in Table 1 and as part of the metabolic pathway in Fig. 2. The relative factor-scores of the first three factors classified the four treatments into groups, which in turn were related to disease progress to assign plant–pathogen interaction function to a factor-vector. The sets of metabolites with significant factor-loadings to
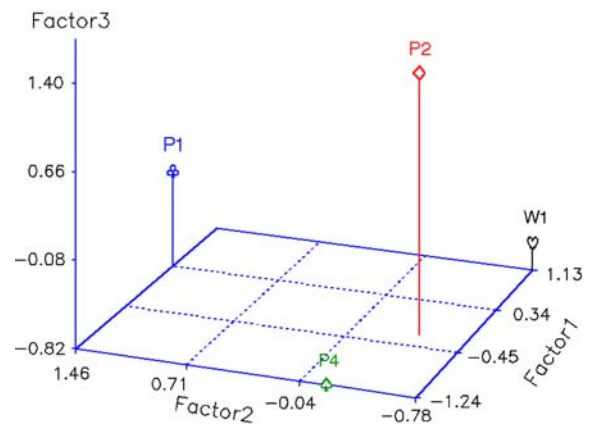
Fig. 1 Scatter plot of treatments using factor scores based on factor analysis of the abundances of 106 metabolites. The treatments are: Water-inoculated 1 DAI (W1 = ♥), Pathogen-inoculated 1, 2 and 4 DAI (P1 = ♣, P2 = ♦, and P4 = ♠), respectively. The factors explained the plausible underneath functions (Treatments with the highest F-scores); Treatments with F1-scores in descending order are: W1 > P1 > P2 > P4 = Homeostasis state of plant (no stress); Treatments with F2-scores in descending order are: P1 > P4 > P2 > W1 = Primary defence response; Treatments with F3 scores in descending order are: P2 > P1 > W1 > P4 = Secondary defence response; Treatments with all negative F-scores F1,2,3 = P4 (Collapse of the defence response). The metabolites differentially and significantly loaded to different factors are given in Table 1

each factor-vector were used to explain the plausible plant–pathogen interaction functions.

Factor 1. Homeostasis or no pathogen stress = W1

The treatments in a descending order of F1-scores were: W1 > P1 > P2 > P4 (Fig. 1). The treatment W1 = at 1 DAI, had the highest positive F1 score, and accordingly the compounds with high loading to F1-vector were used to mainly explain the normal plant function or the homeostasis. 33 metabolites had significant factor-loadings to F1 vector (Factor-loadings > +0.50; Table 1), with 11 SRs (in descending order of factor-loading = 69, 61, 74, 75, 63, 67, 60, 66, 77, 76, and 71), 8 OAs (32, 31, 33, 23, 35, 36, 26, and 37), 4 FAs (45, 44, 43, 42), 2 AAs (3, 14), 5 unidentified (UI) (101, 105, 98, 102, and 106) and 3 other groups (OG) (80, 90, and 84). Of these metabolites, 13 were PR-metabolites. Relatively higher abundances of these metabolites were associated with homeostasis (W1) while the lower

Fig. 2 Metabolic pathways of the potato cv. AC Novachip inoculated with *P. infestans*. The Factor loadings of metabolites to F1; F2; F3 vectors are given in the pathway, below the metabolites that were detected in this study. Boxes = detected amino acids; Ellipses = metabolic pathways; F1 = Homeostasis; F2 = Primary defence response; F3 = Secondary defence response; All 3 factor vectors low = Collapse of defence. EC = Enzyme commission number according to the Nomenclature Committee of the International Union of Biochemistry and Molecular Biology (NC-IUBMB). DAHP = 3-deoxy-D-arabino-heptulosonate-7-phosphate

abundances with other treatments, especially, pathogenicity (P4).

Factor 2. Primary defence response or initial infection = P1

The treatments in a descending order of F2-scores were: P1 > P4 > P2 > W1 (Fig. 1). The treatment P1 = at 1 DAI, had the highest F2-score and accordingly the metabolites with significant loadings to F2, which included several plant defence-related metabolites, were considered to explain the primary defence response. Thirty-four metabolites loaded significantly to F2, including 9 AA (1, 2, 10, 11, 3, 4, 5, 6, and 12), 7 OA (15, 16, 17, 26, 25, 27, and 28), 7 FA (48, 49, 39, 40, 41, 50, and 42), 2 SR (64, 65), 6 OG (85, 80, 82, 83, 79, and 84), and 3 UI (96, 97, and 98). A positive strong association between the significantly up-regulated metabolites and high loadings to F2 was found. According to ANOVA results, only 18 of these 34 metabolites were PR-metabolites consisting of 6 AA (1, 2, 3, 4, 5, and 6), 4 FA (39, 40, 41 and 42), 3 OA (15, 16, and 17), 3 UI (96, 97 and 98), and 2 OG (79 and 80). Relatively higher abundances of these metabolites were associated with primary defence (P1) while lower abundances with other treatments, especially, homeostasis (W1).

Factor 3. Secondary defence response or advanced infection = P2

The treatments in a descending order of F3-scores were: P2 > P1 > W1 > P4 (Fig. 1). The treatment P2 = at 2 DAI, had the highest F3-score, and

accordingly the metabolites with significant loadings to F3, which included several plant PR-metabolites, were used to explain the secondary defence response. Thirty-three metabolites loaded significantly to F3, including 7 FA (54, 46, 53, 57, 50, 55, and 41), 6 AA (7, 9, 5, 8, 12, and 6), 6 OA (30, 18, 27, 28, 19, and 16), 4 SR (68, 70, 71, and 65), 5 UI (99, 103, 104, 97, and 100) and 5 OG (93, 81, 85, 79, and 90). Of these metabolites, 15 were PR-metabolites including 5 AA (7, 9, 5, 8, and 6), 3 OA (18, 19 and 16), 2 FA (46, and 41), 3 UI (99, 97, and 100), and 2 OG (81, and 79). Relatively higher abundances of these metabolites were associated with secondary defence (P2) while the lower abundances with other treatments.

Factors 1–3. Collapse of the primary and secondary defence responses or disease establishment = P4

The treatment P4 = at 4 DAI, had the lowest scores for all the three factors and accordingly the metabolites with significantly negative factor-loadings, included negative factor-loading of defence-related metabolites, were used to explain the function of collapse of defence responses. Only 6 metabolites including 2 OA (34, and 24), 2 FA (56, and 59), and 2 SR (72, and 78) had negative loading to F1, F2, F3 and their P/W ratios were: P4/W > P2/W > P1/W. Among the metabolites significantly loaded, only L-Gluconic acid (24) was a PR-metabolite.

Discussion

A total of 106 metabolites, including 42 PR-metabolites, were tentatively identified from potato leaves inoculated with the late blight pathogen. This is the first report of PR-metabolites in the potato-late blight interaction following metabolomics approach. The ANOVA and Duncan's multiple range tests were used to compare the abundances of individual metabolites among treatments. The FACTOR analysis was used to extract the hidden functions of sets of correlated metabolites. FACTOR analysis was superior to ANOVA in explaining the correlations and functions of metabolites within and among different treatments. For example, the AA L-serine (10) was not significantly different according to ANOVA even though it was highly up-regulated in P1/W1, P2/W

and P4/W1 with 2.88, 2.22 and 2.04 folds, respectively. The biological variations among blocks (replicates over time) were high and masked the effect of treatments for several metabolites. According to FACTOR analysis, L-serine loaded highly to F2 (that explained the primary defence response as will be discussed later). The same trend was seen in several metabolites such as 11, 12, 27, 30, 31, 49, 50, 53, 64, 65, 70, 82, 83, 85,103 and 104 in which the abundances were not significant based on ANOVA, but FACTOR analysis was able to assign them to biological functions. Therefore, the best of both analyses was used to explain the plant–pathogen interactions in P1, P2, and P4, with more emphasis on FACTOR analysis to explain biological functions and the plausible activated metabolic pathways of the diseased potato leaves.

FACTOR analysis identified several metabolites associated with different factor-vectors, which in turn classified the four treatments (W1, P1, P2 and P4). The factor-vectors classified the treatments into metabolic clusters, which were related to disease progress to identify plant–pathogen interaction functions, which in turn were explained based on sets of metabolites loading to these factor-vectors: (i) homeostasis; (ii) primary defence against pathogen attack; (iii) secondary defence against pathogen attack; (iv) collapse of the host defence. The up or down-regulation of the PR-metabolites were further used to explain the role of metabolites in plant defence and also the plausible 'scale-free' satellite-metabolic-network of plant following pathogen invasion (Barabasi and Oltvai 2004) using metabolic pathway bioinformatics resources, Kyoto Encyclopedia of Genes and Genomes (KEGG) (http://www.genome.jp/kegg/), and Metabolic Pathways of the Diseased Potato (http://www.scri.sari.ac.uk/TiPP/pps/Chart.pdf). Several metabolites, previously known to be associated with biotic stresses of plants, were significantly up-regulated 24 and 48 h following pathogen inoculation, while the abundances of these metabolites decreased in 96 h, indicating the collapse of the primary and secondary defence responses. Even though the host-pathogen interactions are quite complex, the temporal dynamics of metabolites detected here following pathogen inoculation, types and abundances, were able to explain plant pathogenesis and defence responses.

Homeostasis (F1 = W1)

The F1 appears to mainly explain the non-stressed or homeostasis state of the plant, where the plant produces sugars through photosynthesis that are utilized to supply essential energy for plant growth and the excess sugars are stored for future use. The homeostasis conditions require the coordination and activation of several metabolic pathways that work in complete harmony. Some of the amino acids detected at 1 DAI, in addition to their role in the production of small molecular weight defence compounds such as phenols, flavones, coumarines, nitrogen and sulphur containing anti-microbial and insect deterrent compounds such as glucosinolates and glycosides (Osbourn 1996), are also important in the production of structural proteins such as microfilaments or actin filaments that are reported to be involved in the defence response against *P. infestans* attack (Furuse et al. 1999). Furthermore, they are important in the production of microtubules, enzymes and PR-proteins that play important roles in plant–pathogen interactions (Van Loon and Van Strien 1999).

Fatty acids are major components of the triglycerides, cutin, suberin, and waxes, plasma, plastid and mitochondrial membranes (Somerville et al. 2000).The unsaturated FAs are the basic components of the membrane lipids and make about 70% of the membrane lipids of the chloroplasts (Yaeno et al. 2004). In Water treatment, all of the 4 FAs that loaded highly to F1 (homeostasis) were unsaturated. However, following pathogen invasion, over time, their total abundances were reduced. In these cases, either the production of the unsaturated FAs was reduced, as a result of the malfunctioning of the chloroplasts due to pathogen infection (Soulie et al. 1989) or the utilization of the unsaturated FAs was increased.

Primary defence (F2 = P1)

Following pathogen attack, only few sugars loaded significantly either to the primary or to the secondary defence responses of the plant. D-Glucose (63) and two unidentified metabolites (101 and 102; appear to be sugars) were down-regulated in treatments following pathogen inoculation. Broeckling et al. (2005) found that the carbon resources of the plant, especially sucrose, were highly reduced after the exposure of cell culture of *Medicago truncatula* to

different elicitors including yeast, methyl jasmonate and UV light. Sugars are precursors of many metabolic pathways and are the building blocks of cell wall middle lamellae, and participate in the post-modification of proteins and fatty acids. Moreover, they are important in the production of structural defence materials such as callose and papillae in response to pathogen attack. The deposition of callose ((1–3) β-D-glucan chains) following infection by *P. infestans* in clones of *Solanum* has been reported (Vleeshouwers et al. 2000). The callose accumulation is mainly associated with the deposition of papillae and was reported in biotrophic and hemibiotrophic fungi and preceded the hypersensitive response (Schmelzer 2002). On the other hand, dramatic temporal changes in the amino acids were noticed following pathogen inoculation. Amino acids belonging to different AAs families were up-regulated. Different AAs from aspartate, glutamine, alanine and aromatic families were found to be significantly activated mainly at the first day after pathogen inoculation. These AAs loaded significantly to F2, indicating a primary defence response against *P. infestans* attack (Fig. 2).

The aspartic acid family of amino acids is produced from the dicarboxylic acid precursor oxaloacetate (OAA) (Fig. 2). The plant mainly produces oxaloacetate via two well studied pathways. The citric acid pathway (Tricarboxylic acid, TCA-cycle) occurs in the mitochondria in which oxaloacetate is produced from the precursor malate with the help of the mitochondrial isoenzyme malate dehydrogenase (EC: 1.1.1.37; KEGG). A second pathway is the production of OAA in the plant cytosol from phosphoenolpyruvate (PEP) with the help of the enzyme PEP carboxylase (EC: 4.1.1.31; KEGG). The OAA produced is then converted to malate with the help of the cytosolic enzyme malate dehydrogenase (EC: 1.1.1.37; KEGG). The dicarboxylic organic acid, fumarate, is the precursor of malate in the TCA cycle. Following pathogen inoculation, the two organic acids fumarate (25) and succinate (26) were not significantly up-regulated according to ANOVA results but both had F2 loadings of 0.74. Therefore, it is more likely that OAA, the precursor of the aspartic acid, was mainly produced in the plant cytosol. Aspartic acid is the primary block for the production of other AAs of this family. A metabolic pathway that leads to the synthesis of threonine and isoleucine was

found to be highly up-regulated in P1, with high loadings to F2 vector. Cystathionine (92), a precursor of methionine was neither significantly up- nor down-regulated and had very low loadings to F2 of 0.06. Thus, in conclusion, one branch of the aspartic acid family that produces L-threonine (2) and L-isoleucine (6) was mainly up-regulated in P1, at 1 DAI and had high loadings to F2.

The AAs of the alanine family are produced from the precursor pyruvic acid. Compared to other treatments, the AAs alanine (3) and valine (5) were significantly up-regulated in P1 and had high loadings to F2. The AAs valine and Isoleucine (discussed earlier) have similar metabolic pathways in the chloroplasts and were up-regulated following pathogen inoculation. These AAs share four common enzymes during their synthesis namely acetohydroxy acid synthase (EC: 2.2.1.6; KEGG), ketol-acid reductoisomerase (EC: 1.1.1.86; KEGG), dihydroxy-acid dehydratase (EC: 4.2.1.9; KEGG) and aminotransferase (EC: 2.6.1.42; KEGG) (Fig. 2). The AAs valine, Isoleucine and leucine are important in the production of plant defence secondary metabolites such as cyanogenic glycosides, and glucosinolates (Coruzzi and Last 2000). The serine family AAs (L-serine and glycine) are produced from the precursor 3-phosphoglycerate. The AAs L-serine (10) had high loadings to F2 of 0.84 and was up-regulated with (P1/W = 2.88) > (P2/W = 2.22) > (P4/W = 2.04) but according to ANOVA tests the four treatments (W, P1, P2 and P4) were not significantly different.

The fatty acid, Stearic acid (50; C18:0) had high factor-loadings to F2 and F3 (P1 and P2). This FA can be desaturated by the enzyme 9-desaturase to produce oleic acid (41; C18:1) which was significantly up-regulated in P1 and P2, with P1/W > P2/W > P4/W. Oleic acid (41) either undergoes desaturation with the help of the enzyme 12-desaturase to produce linoleic acid (40; C18:2) or hydroxylated with the help of epoxygenase and Cyt. P-450 enzymes to produce different cutin monomers. The FA Linoleic acid (40; C18:2) had high factor-loading to F2 (P1 treatment). This FA could be further modified by 9- or 13-lipoxygenases to produce different FAs monomers or it might be directly desaturated by the enzyme 15-desaturase to produce linolenic acid (43; C18:3) (http://www.scri.sari.ac.uk/TiPP/pps/Chart.pdf). Linolenic acid (43; C18:3) was found to be significantly down-regulated in P4

treatment. This FA is the primary block in the oxylipin pathway and that produces many jasmonates (oxylipins) and jasmonic acid, a signal molecule involved directly in the defence response against insects and pathogens (Weber 2002; Somerville et al. 2000).

The glycoalkaloid metabolite, solanidine (79) had high factor-loadings to F2 and F3-scores with P1/W > P2/W > P4/W. This metabolite was reported to have anti-microbial activity (Lachman et al. 2001; Moehs et al. 1997) and is produced from the cytocylic acetyl-CoA through the mevalonate pathway (Fig. 2). Acetyl-CoA in the cytosol can be produced from the organic acid citrate by the enzyme ATP-citrate lyase (Fatland et al. 2005).

The OAs α-Ketoglutarate is a precursor of the glutamate family AAs. The conversion of the AA L-Glutamic acid to L-proline (12) involves many steps and intermediates. The AA glutamine (8) was significantly up-regulated in P1, P2 and P4. The AA L-proline derivative (4) was found to be significantly up-regulated in P1 with a loading value of 0.76 to F2. On the contrary, L-proline (12) was not significantly up-regulated according to ANOVA tests but had high loading values of 0.52 and 0.62 for both F2 and F3, respectively. L-proline is an important precursor in the production of cell wall proteins, i.e. proline-rich proteins (PRPs) and hydroxyproline-rich glycoproteins (HRGPs) (Showalter 1993). Extensin, a subgroup of HRGPs family, is known for its ability to cross-link and is covalently linked to different cell wall components such as pectin. This increases the mechanical strength and rigidity of the plant cell walls (Jackson et al. 2001). Higher amount of the AAs glutamine, arginine and proline (glutamate family AAs) as well as the AAs asparagine and lysine (aspartate family AAs) were found in vitro-grown potato tubers compared to soil-grown tubers (Roessner et al. 2000). Also, an increase in glutamine, glutamate and asparagine amino acids were reported in water stressed tomato leaves (Bauer et al. 1997).

Secondary defence phase (F3 = P2)

On the second day after pathogen inoculation, the aromatic amino acids (tyrosine (7) and L-phenylalanine (9)), Glutamine (8), L-isoleucine (6) and L-valine (5) were significantly up-regulated and had high loadings to F3 indicating a secondary defence

response against *P. infestans*. Noticeably, all these AAs were found to be significantly up-regulated in P1 except the aromatic AA L-phenylalanine (9) that was only up-regulated in P2. Both AAs L-phenylalanine (9) and L-Tyrosine (7) had high loadings to F3 of (0.79 and 0.86, respectively). The primary precursors of these aromatic AAs are phosphoenolpyruvate and erythrose-4-phosphate that combine together to produce the organic acids shikimate and later chorismate (Fig. 2). Two separate pathways are involved in the production of the aromatic AAs. One pathway activates the production of both tyrosine and phenylalanine, and the second pathway produces tryptophan. The enzyme chorismate mutase (EC: 5.4.99.5; KEGG) converts chorismate to prephenate then to phenylalanine and /or tyrosine with the help of different enzymes (Coruzzi and Last 2000). Tyrosine and phenylalanine are the primary precursors of a wide range of secondary metabolites such as phenolics, coumarines, flavones, isoflavones, isoflavanones, lignins, tannins, and the secondary messenger salicylic acid and many others (Fig. 2). These metabolites are very important in the defence response against pathogens and the signal molecules can activate several defence pathways leading to more complex defence (Dixon et al. 2002; Barabasi and Oltvai 2004). In P2 both D-Gluconic acid (22) and Xylulose (62), were up-regulated, though it was less than P4/W (Table 1). These metabolites are members of the Pentose Phosphate Pathway (PPP) that supplies the precursor erythrose-4-phosphate that is essential in the aromatic AAs synthesis. Relative to P2, in P1, most of the phosphoenolpyruvate (PEP) might have been primarily used to produce either pyruvate, the precursor of the alanine family, or OAA, the precursor of the aspartate family. These two families were less up-regulated in P2 as compared to P1 and that could be the main reason that made PEP more available for the production of more aromatic amino acids in P2. Accordingly, it appears that the PPP and the aromatic AAs pathways were highly activated in P2.

Collapse of the defence (negative loadings to all three factor vectors = P4)

Six metabolites including 2 OA (34, and 24), 2 FA (56, and 59), and 2 SR (72 and 78) had negative loading to F1, F2, F3, and their P/W ratios were:

P4/W > P2/W > P1/W. Among the metabolites significantly loaded, only L-Gluconic acid was a PR-metabolite. In P4, many of the reported OAs and all the AAs belonging to aromatic, glutamate, alanine, and aspartate families were down-regulated compared to P1 or P2 except Glutamine (8). This indicates the reduction in the synthesis of these PR-metabolites and the collapse of the primary and secondary defence responses. The P4/W ratios of the un-saturated FAs were the lowest among treatments. This reduction in the P4/W ratios accompanied the collapse of primary and secondary defence responses of the plant.

The FA 7,10,13-Hexadecatrienoic acid (44; C16:3) that loaded highly to W1 was neither up-regulated nor down-regulated in P1, but was significantly down-regulated in P2 and P4. This FA is a precursor of dinor-oxo-phytodienoic acid (dnOPDA), a potential wound-signaling metabolite (Weber et al. 1997; Weber 2002; http://www.scri.sari.ac.uk/TiPP/pps/Chart.pdf). The FA 7,10-Hexadecadienoic acid (45) might be a precursor of the FA 7,10,13-Hexadecatrienoic acid and was found also to be significantly down-regulated in P2 and P4.

The FA Linolenic acid (C18:3) that loaded highly to W1 (homeostasis) was neither up-regulated nor down-regulated in P1 and was down-regulated in P2 and P4. This FA is a potential precursor for the production of the signaling metabolite jasmonic acid and its derivatives, which are known to activate different plant defence responses (Liechti and Farmer 2002).

In this study, the GC/MS technology platform was used for metabolite profiling because of its known sensitivity and selectivity, and also is considered as the most common platform among researchers for studying the plant metabolome (Dunn et al. 2005; Sumner et al. 2003). Although the number of metabolites detected and tentatively identified was small, the results showed the capability of metabolite profiling and multivariate analyses to identify hidden plant–pathogen interaction functions. According to FACTOR analysis, the plant primary defence response at 1 DAI was considered to be mainly due to an increase in the production of several AAs including those belonging to Serine, Aspartate, and Alanine families and many OAs (high loadings to F2; Fig. 2). Activation of these metabolites occurred in different satellites or neurons of network of

pathways. On the other hand, at 2 DAI (P2), the pathways activated were different from those in 1 DAI (P1) where glutamate, L-isoleucine, L-valine and the aromatic AAs phenylalanine and tyrosine, the primary blocks of the phenylpropanoid pathway, and the C16 FAs that activate the wound signaling response of the plant were activated. At 4 DAI the primary and the secondary plant defence responses collapsed and the P4/W ratios were the lowest for several AAs, FAs and OAs. At this stage the plant primary and secondary defence responses were failing and the plant was not able to stop the necrotrophic phase of the pathogen that usually takes place 2–3 DAI (Vleeshouwers et al. 2000). These findings indicate the potential application of metabolic profiling technology and multivariate analyses to identify hidden functions of plant defence and the plausible network of metabolic pathways that produce several metabolites, including some that are known to have antimicrobial activity or lead to their production. Similar studies on different potato breeding lines with varying levels of horizontal resistance or quantitative trait loci (QTL) against late blight could lead to metabolite phenotyping of cultivars and high throughput screen for disease resistance.

References

Barabasi, A. L., & Oltvai, Z. N. (2004). Network biology: Understanding the cell's functional organization. *Nature Reviews Genetics, 5*, 101–113.

Bauer, D., Biehler, K., Fock, H., Carrayol, E., Hirel, B., Migge, A., & Becker, T. W. (1997). A role for cytosolic glutamine synthetase in remobilization of leaf nitrogen during water stress in tomato. *Physiologia Plantarum, 99*, 241–248.

Bino, R. J., Hall, R. D., Fiehn, O., Kopka, J., Saito, K., Draper, J., Nikolau, B. J., Mendes, P., Roessner-Tunali, U., Beale, M. H., Trethewey, R. N., Lange, B. M., Wurtele, E. S., & Sumner, L. W. (2004). Potential of metabolomics as a functional genomics tool. *Trends in Plant Science, 9*, 418–425.

Broeckling, C. D., Huhman, D. V., Farag, M. A., Smith, J. T., May, G. D., Mendes, P., Dixon, R. A., & Sumner, L. W. (2005). Metabolic profiling of *Medicago truncatula* cell cultures reveals the effects of biotic and abiotic elicitors

on metabolism. *Journal of Experimental Botany, 56*, 323–336.

Carlisle, D. J., Cooke, L. R., Watson, S., & Brown, A. E. (2002). Foliar aggressiveness of Northern Ireland isolates of *Phytophthora infestans* on detached leaflets of three potato cultivars. *Plant Pathology, 51*, 424–434.

Coruzzi, G., & Last, R. (2000). Amino acids. In B. B. Buchanan, W. Gruissem, & R. Jones (Eds.), *Biochemistry and molecular biology of plants* (pp. 358–410). Rockville, Maryland: American Society of Plant Physiologists.

Daayf, F., & Platt, H. W. (2003). Differential pathogenicity on potato and tomato of *Phytophthora infestans* US-8 and US-11 strains isolated from potato and tomato. *Canadian Journal of Plant Pathology, 25*, 150–154.

Daayf, F., & Platt, H. W. (1999). Assessment of mating types and resistance to metalaxyl of Canadian populations of *Phytophthora infestans* in 1997. *American Journal of Potato Research, 76*, 287–295.

Dixon, R. A., Achnine, L., Kota, P., Liu, C.-J., Reddy, M. S. S., & Wang, L. (2002). The phenylpropanoid pathway and plant defence – a genomic perspective. *Molecular Plant Pathology, 3*, 371–390.

Dunn, W. B., Bailey, N. J. C., & Johnson, H. E. (2005). Measuring of Metabolome: Current analytical technologies. *The Analyst, 130*, 606–625.

Eckel, W. E. (2000). Making sense of non-target compound data from GC-MS library searches. *American Laboratory, 32*, 17–20.

Evers, D., Ghislain, M., Hausman, J.-F., & Dommes, J. (2003). Differential gene expression in two potato lines differing in their resistance to *Phytophthora infestans*. *Journal of Plant Physiology, 160*, 709–712.

Fatland, B. L., Nikolau, B. J., & Wurtele, E. S. (2005). Reverse genetic characterization of cytosolic Acetyl-CoA generation by ATP-citrate in *Arabidopsis*. *The Plant Cell, 17*, 182–203.

Fiehn, O. (2001). Combining genomics, metabolome analysis, and biochemical modeling to understand metabolic networks. *Comparative and Functional Genomics, 2*, 155–168.

Fiehn, O., Kopka, J., Trethewey, R. N., & Willmitzer, L. (2000a). Identification of uncommon plant metabolites based on calculation of elemental compositions using gas chromatography and quadrupole mass spectrometry. *Analytical Chemistry, 72*, 3573–3580.

Fiehn, O., Kopka, J., Dormann, P., Altmann, T., Trethewey, R. N., & Willmitzer, L., (2000b). Metabolite profiling for plant functional genomics. *Nature Biotechnology, 18*, 1157–1161.

Flier, W. G., van de Bosch, G. B. M., & Turkensteen, L. J. (2003). Stability of partial resistance in potato cultivars exposed to aggressive strains of *Phytophthora infestans*. *Plant Pathology, 52*, 326–337.

Furuse, K., Takemoto, D., Doke, N., & Kawakita, K. (1999). Involvement of actin filament association in hypersensitive reactions in potato cells. *Physiological and Molecular Plant Pathology, 54*, 51–61.

Gebhardt, C., & Valkonen, J. P. T. (2001). Organization of genes controlling disease resistance in the potato genome. *Annual Review of Phytopathology, 39*, 79–102.

Hamzehzarghani, H., Kushalappa, A. C., Dion, Y., Rioux, S., Comeau, A., Yaylayan, V., Marshall, W. D., & Mather, D.

E. (2005). Metabolic profiling and factor analysis to discriminate quantitative resistance in wheat cultivars against fusarium head blight. *Physiological and Molecular Plant Pathology, 66*, 119–113.

Jackson, P. A. P., Galinha, C. I. R., Pereira, C. S., Fortunato, A., Soares, N. C., Amancio, S. B. Q., & Ricardo, C. P. P. (2001). Rapid deposition of extensin during the elicitation of grapevine callus cultures is specifically catalyzed by a 40-kilodalton peroxidase. *Plant Physiology, 127*, 1065–1076.

Johnson, H. E., Broadhurst, D., Goodcare, R., & Smith, A. R. (2003). Metabolic fingerprinting of salt-stressed tomatoes. *Phytochemistry, 62*, 919–928.

Johnson, R. A., & Wichern, D. W. (2002). *Applied multivariate statistical analysis*. NJ: Upper Saddle River Prentice Hall.

Khattree, N. R., & Naik, D. N. (2000). *Multivariate data reduction and discrimination with SAS software*. Cary, NC: SAS Institute Inc.

Kombrink, E., & Schmelzer, E. (2001). The hypersensitive response and its role in local and systemic disease resistance. *European Journal of Plant Pathology, 107*, 69–78.

Kopka, J., Schauer, N., Krueger, S., Birkemeyer, C., Usadel, B., Bergmuller, E., Dormann, P., Weckwerth, W., Gibon, Y., Stitt, M., Willmitzer, L., Fernie, A. R., & Steinhauser, D. (2005). GMD@CSBDB: The Golm Metabolome Database. *Bioinformatics, 21*, 1635–1638.

Lachman, j., Hamouz, K., & Pivec, V. (2001). Potato glycoalkaloids and their significance in plant protection and human nutrition—Review. *Series Rostlinna Vyroba, 47*, 181–191.

Lee, M. L., Vassilaros, L., White, C. M., & Novotny, M. (1979). Retention indices for programmed-temperature capillary-column gas chromatography of polycyclic aromatic hydrocarbons. *Analytical Chemistry, 6*, 768–773.

Liechti, R., & Farmer, E. E. (2002). The jasmonate pathway. *Science, 296*, 1694–1650.

Medina, M. V., Platt, H. W., & Peters, R. D. (1999). Severity of late blight tuber infection caused by US-1 and US-8 genotypes of *Phytophthora infestans* in 12 potato cultivars. *Canadian Journal of Plant Pathology, 21*, 388–390.

Moehs, C. P., Allen, P. V., Friedman, F., & Belknap, W. R. (1997). Cloning and expression of solanidine UDP-glucose glucosyltransferase from potato. *The Plant Journal, 11*, 227–236.

Montesano, M., Brader, G., & Palva, E. T. (2003). Pathogen derived elicitors: Searching for receptors in plants. *Molecular Plant Pathology, 4*, 73–79.

Munger, R., Glass, A. D. M., Goodenow, D. B., & Lightfoot, D. A. (2005). Metabolic fingerprinting in transgenic *Nicotiana tabacum* altered by *Escherichia coli* glutamate dehydrogenase gene. *Journal of Biomedicine and Biotechnology, 2005*, 198–214.

Osbourn, A. E. (1996). Preformed antimicrobial compounds and plant defence against fungal attack. *The Plant Cell, 8*, 1821–1831.

Palva, T. K., Holmstrom, K.-O., Heino, P., & Palva, E. T. (1993). Induction of plant defence response by exoenzymes of *Erwinia carotovora* subsp *carotovora*. *Molecular Plant-Microbe Interactions, 6*, 190–196.

Peters, R. D., Forster, H., Platt, H. W., Hall, R., & Coffey, M. D. (2001). Novel genotypes of *Phytophthora infestans* in Canada during 1994 and 1995. *American Journal of Potato Research, 78*, 39–45.

Peters, R. D., Platt, H. W., Hall, R., & Medina, M. (1999). Variation in aggressiveness of Canadian isolates of *Phytophthora infestans* as indicated by their relative abilities to cause potato tuber rot. *Plant Disease, 83*, 652–661.

Roessner, U., Wagner, C., Kopka, J., Trethewey, R. N., & Willmitzer, L. (2000). Simultaneous analysis of metabolites in potato tuber by gas chromatography-mass spectrometry. *The Plant Journal, 23*, 131–142.

Roessner, U., Willmitzer, L., & Fernie, A. R. (2001). High-resolution metabolic phenotyping of genetically and environmentally diverse potato tuber systems. Identification of phenocopies. *Plant Physiology, 127*, 749–764.

Schmelzer, E (2002). Cell polarization, a crucial process in fungal defence. *Trends in Plant Science, 7*, 411–415.

Showalter, A. M. (1993). Structure and function of plant cell wall proteins. *Plant Cell, 5*, 9–23.

Simmonds, N. W., & Wastie, R. L. (1987). Assessment of horizontal resistance to late blight of potatoes. *Annals of Applied Biology, 111*, 213–221.

Somerville, C., Browse, J., Jaworski, J., & Ohlrogge, J. B. (2000). Lipids. In B. B. Buchanan, W. Gruissem, & R. Jones (Eds.), *Biochemistry and molecular biology of plants* (pp. 456–527). Rockville, Maryland: American Society of Plant Physiologists.

Soulie, M. C., Troton, D., Malfatti, P., Bompeix, G., & Laval-Martin, D. (1989). Postinfectional changes of lipids and photosynthesis in *Lycopersicon esculentum* susceptible to *Phytophthora capasi*. *Plant Science, 61*, 169–178.

Stromberg, A., Bostrom, U., & Hallenberg, N. (2001). Oospore germination and formation by the late blight pathogen *Phytophthora infestans in vitro* and under field conditions. *Journal of Phytopathology, 149*, 659–664.

Sumner, L. W., Mendesb, P., & Dixon, R. A. (2003). Plant metabolomics: Large-scale phytochemistry in the functional genomics era. *Phytochemistry, 62*, 817–836.

Van Loon, L. C., & Van Strien, E. A. (1999). The families of pathogenesis-related proteins, their activities, and comparative analysis of PR-1 type proteins. *Physiological and Molecular Plant Pathology, 55*, 85–97.

Vleeshouwers, V. G. A. A., van Dooijeweert, W., Govers, F., Kamoun, S., & Colon, L. T. (2000). The hypersensitive response is associated with host and nonhost resistance to *Phytophthora infestans*. *Planta, 210*, 853–864.

Wastie, R. L. (1991). Breeding for resistance. In D. S. Ingram, & P. H. Williams (Eds.), *Phytophthora infestans, the cause of late blight of potato. Advances in plant pathology* (Vol. 7, pp. 193–223). London, UK: Academic Press.

Weber, H. (2002). Fatty acid-derived signals in plants. *Trends in Plant Science, 7*, 217–224.

Weber, H., Vick, B. A., & Farmer, E. E. (1997). Dinor-oxo-phytodienoic acid: A new hexadecanoid signal in the jasmonate family. *Proceedings of the National Academy of Science of the USA, 94*, 10473–10478.

Yaeno, T., Matsuda, O., & Iba, K. (2004). Role of chloroplast trienoic fatty acids in plant disease defence responses. *The Plant Journal, 40*, 931–941.